

Resummation of Relativistic Corrections to $e^+e^- \rightarrow J/\psi + \eta_c$

Geoffrey T. Bodwin,¹ Jungil Lee,^{1,2} and Chaehyun Yu²

¹ *High Energy Physics Division, Argonne National Laboratory,
9700 S. Cass Avenue, Argonne, Illinois 60439, USA*

² *Department of Physics, Korea University, Seoul 136-701, Korea*

Abstract

We present a new calculation, in the nonrelativistic QCD (NRQCD) factorization formalism, of the relativistic corrections to the double-charmonium cross section $\sigma[e^+e^- \rightarrow J/\psi + \eta_c]$ at the energy of the Belle and BABAR experiments. In comparison with previous work, our calculation contains several refinements. These include the use of the improved results for the nonperturbative NRQCD matrix elements, the resummation of a class of relativistic corrections, the use of the vector-meson-dominance method to calculate the fragmentation contribution to the pure QED amplitude, the inclusion of the effects of the running of α , and the inclusion of the contribution that arises from the interference between the relativistic corrections and the corrections of next-to-leading order in α_s . We also present a detailed estimate of the theoretical uncertainty. We conclude that the discrepancy between the theoretical prediction for $\sigma[e^+e^- \rightarrow J/\psi + \eta_c]$ and the experimental measurements has been resolved.

PACS numbers: 12.38.-t, 12.39.St, 12.40.Vv, 13.66.Bc

I. INTRODUCTION

For a number of years, one of the largest discrepancies in the standard model has been the disagreement between theory and experiment for exclusive double-charmonium process $e^+e^- \rightarrow J/\psi + \eta_c$ at the B -factory energy of 10.58 GeV. Initially, the Belle Collaboration reported for the cross section times the branching fraction into four or more charged tracks $\sigma[e^+e^- \rightarrow J/\psi + \eta_c] \times B_{\geq 4} = 33_{-6}^{+7} \pm 9$ fb (Ref. [1]). The first theoretical predictions were based on NRQCD factorization calculations [2] at leading order in α_s , the QCD coupling constant, and v , the heavy-quark (or antiquark) velocity in the quarkonium rest frame. These predictions were $\sigma[e^+e^- \rightarrow J/\psi + \eta_c] = 3.78 \pm 1.26$ fb (Ref. [3]) and $\sigma[e^+e^- \rightarrow J/\psi + \eta_c] = 5.5$ fb (Ref. [4]).¹ The calculation of Ref. [3] includes QED effects, while that of Ref. [4] does not. Other differences between these calculations arise from different choices of the charm-quark mass m_c , NRQCD matrix elements, and α_s . The sensitivities of the calculations to these choices are indicative of large sources of uncertainty in the theoretical calculations that have not yet been quantified.

More recently, the Belle Collaboration has measured the production cross section times the branching fraction into more than two charged tracks and finds that $\sigma[e^+e^- \rightarrow J/\psi + \eta_c] \times B_{>2} = 25.6 \pm 2.8 \pm 3.4$ fb (Ref. [5]). BABAR Collaboration has also measured this quantity, and obtains $\sigma[e^+e^- \rightarrow J/\psi + \eta_c] \times B_{>2} = 17.6 \pm 2.8 \pm 2.1$ fb (Ref. [6]). These new experimental results have narrowed the gap between theory and experiment.

An important recent theoretical development is the calculation of the corrections of next-to-leading order (NLO) in α_s (Ref. [7]). These yield a K factor of about 1.96. While this K factor is substantial, it does not, by itself, completely remove the discrepancy between theory and experiment.

Relativistic corrections to $\sigma[e^+e^- \rightarrow J/\psi + \eta_c]$ also make a significant contribution to the theoretical prediction. These corrections arise in two ways. First, they appear directly in the corrections of order v^2 and higher to the process $e^+e^- \rightarrow J/\psi + \eta_c$ itself. Second, they arise indirectly when one makes use of phenomenological determinations of certain NRQCD matrix elements that appear in the expression for $\sigma[e^+e^- \rightarrow J/\psi + \eta_c]$. For example, the relevant matrix element of leading order in v for the J/ψ can be determined phenomenologically

¹ The authors of Ref. [3] initially reported a cross section of 2.31 ± 1.09 fb, but later corrected a sign error in the QED interference term to arrive at the value cited above.

from the experimental value for the width for $J/\psi \rightarrow e^+e^-$ and the theoretical expression for that process. However, the theoretical expression contains relativistic corrections, which then indirectly affect the calculation of $\sigma[e^+e^- \rightarrow J/\psi + \eta_c]$. The first relativistic correction appears at order v^2 . ($v^2 \approx 0.3$ for charmonium.) In Ref. [3], the order- v^2 correction was calculated and was found to be about $1.95\langle v^2 \rangle_{J/\psi} + 2.37\langle v^2 \rangle_{\eta_c}$. Here, $\langle v^2 \rangle_H$ is the ratio of an order- v^2 nonperturbative NRQCD matrix element to the leading-order matrix element in the quarkonium state H . The large coefficients in the order- v^2 correction potentially lead to a relativistic correction. In Ref. [3], the K factor for the relativistic corrections was found to be $2.0^{+10.9}_{-1.1}$. The large uncertainties arose from large uncertainties in the NRQCD matrix elements.

Recently, progress has been made in reducing the uncertainties in the order- v^2 NRQCD matrix elements by making use of a potential model to calculate the quarkonium wave function [8]. The results of Ref. [8] allow one to make a meaningful prediction for the relativistic corrections to $\sigma[e^+e^- \rightarrow J/\psi + \eta_c]$. Making use of these results to compute the relativistic corrections and taking into account the corrections of NLO in α_s , the authors of Ref. [9] have given the prediction $\sigma[e^+e^- \rightarrow J/\psi + \eta_c] = 17.5 \pm 5.7$ fb.

The authors of Ref. [10] have taken a different approach, determining the NRQCD matrix elements of leading order in v and of relative order v^2 by using $\Gamma[J/\psi \rightarrow e^+e^-]$, $\Gamma[\eta_c \rightarrow \gamma\gamma]$, and $\Gamma[J/\psi \rightarrow \text{light hadrons}]$ as inputs. Their result, $\sigma[e^+e^- \rightarrow J/\psi + \eta_c] = 20.04$ fb, is in agreement with the result of Ref. [9]. However, as we shall discuss, the values of the individual matrix elements that were used in Ref. [10] differ significantly from the values that were used in Ref. [9].

The results of Refs. [9] and [10] suggest that there is no longer a discrepancy between the experimental measurements and the theoretical prediction. Nevertheless, it is useful to include further refinements that improve the precision of the theoretical prediction and to estimate as precisely as possible the various theoretical uncertainties.

In the present paper, we carry out a new calculation of the relativistic corrections to $\sigma[e^+e^- \rightarrow J/\psi + \eta_c]$. We include the effects of pure QED processes, as well as QCD processes. In the case of the pure QED processes, we incorporate a further refinement by making use of the vector-meson-dominance (VMD) formalism to compute the photon-fragmentation contribution. This approach reduces the theoretical uncertainties that are associated with the pure QED contribution. In our calculation, we make use of the approach of Ref. [8] to

resum a class of relativistic corrections to all orders in v . We also compute the contribution that arises from the interference between the relativistic corrections and the corrections of NLO in α_s . Our calculation takes advantage of the new higher-precision determinations of the relevant NRQCD matrix elements in Ref. [11]. We make use of the detailed error analysis of Ref. [11] to estimate the theoretical uncertainties in our calculation, some of which are highly correlated.

The remainder of this paper is organized as follows. In Sec. II, we discuss the general form of the amplitude for the process $e^+e^- \rightarrow J/\psi + \eta_c$, and, in Sec. III, we discuss the corresponding quark-level amplitude. Sec. IV contains the expression for the NRQCD expansion of the amplitude and a discussion of the matching between NRQCD and full QCD. In Sec. V, we describe the resummation method that we employ. Sec. VI contains the specifics of the frame and coordinate system that we use in the calculation. We present explicit formulas for the cross section in Sec. VII. The VMD method for computing the fragmentation contribution to the pure QED amplitude is summarized in Sec. VIII. We specify how we choose quarkonium masses in the calculation in Sec. IX. We present the method that we use to compute the interference between the relativistic corrections and the corrections of NLO in α_s in Sec. X. We give our numerical results in Sec. XI and compare them with the results from previous calculations in Sec. XII. Finally, we summarize and discuss our results in Sec. XIII.

II. GENERAL FORM OF THE AMPLITUDE FOR $e^+e^- \rightarrow J/\psi + \eta_c$

Let us consider the amplitude for the exclusive process $\gamma^* \rightarrow J/\psi(P_1, \lambda) + \eta_c(P_2)$, where λ is the helicity of the J/ψ . The S -matrix element for $e^+(k_2)e^-(k_1) \rightarrow J/\psi(P_1, \lambda) + \eta_c(P_2)$ can be written as

$$\mathcal{M}(\lambda) = L^\mu \mathcal{A}_\mu[J/\psi(\lambda) + \eta_c], \quad (1)$$

where the leptonic factor L^μ is defined by

$$L^\mu = -i \frac{e_c e^2}{s} \bar{v}(k_2) \gamma^\mu u(k_1). \quad (2)$$

Here, e_c is the fractional electric charge of the charm quark and $s = 4E_{\text{beam}}^2$ is the square of the e^+e^- center-of-momentum (CM) energy. $\mathcal{A}_\mu[J/\psi(\lambda) + \eta_c]$ in Eq. (1) is the vacuum-to- $J/\psi + \eta_c$ matrix element. It can be expressed in the following form, which derives from the

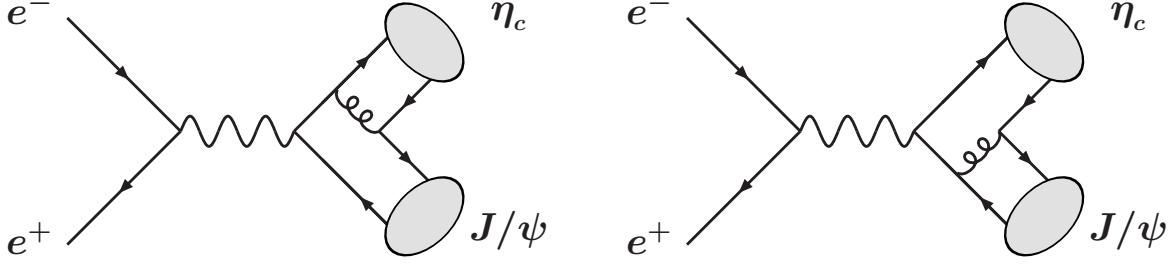


FIG. 1: Feynman diagrams for the process $e^+e^- \rightarrow J/\psi + \eta_c$ at leading order in α_s . The wavy line represents a photon, the curly line represents a gluon, and the straight lines represent the leptons and heavy quarks. There are six additional diagrams that can be obtained by reversing the directions of the arrows on the heavy-quark lines and/or by replacing the gluon by a photon.

Lorentz invariance of the amplitude and the parity conservation of the strong and electromagnetic interactions [3]:

$$\mathcal{A}_\mu[J/\psi(\lambda) + \eta_c] = \langle J/\psi(P_1, \lambda) + \eta_c(P_2) | J_\mu(0) | 0 \rangle = iA\epsilon_{\mu\nu\alpha\beta}P_1^\nu P_2^\alpha \epsilon^{*\beta}(\lambda), \quad (3)$$

where $J_\mu(0)$ is the electromagnetic current, $\epsilon^*(\lambda)$ is the polarization four-vector of the J/ψ with helicity λ whose components in the J/ψ rest frame are $\epsilon^*(\lambda) = [0, \boldsymbol{\epsilon}^*(\lambda)]$. The convention for the antisymmetric tensor in Eq. (3) is chosen so that $\epsilon_{0123} = +1$. We note that A is parity invariant and that \mathcal{A}^μ transforms as a four-vector under parity.

III. AMPLITUDE FOR $\gamma^* \rightarrow Q\bar{Q}(^3S_1) + Q\bar{Q}(^1S_0)$

The exclusive process $\gamma^* \rightarrow J/\psi(P_1, \lambda) + \eta_c(P_2)$ involves the decay of a virtual photon into two heavy quark-antiquark ($Q\bar{Q}$) pairs $Q(p_i)\bar{Q}(\bar{p}_i)$ ($i = 1$ or 2). Both of the pairs are in color-singlet states. At leading order in α_s , the process proceeds through the diagrams shown in Fig. 1, plus two additional diagrams in which the directions of the arrows on the heavy-quark lines are reversed. There are also purely electromagnetic contributions to the process. At leading order in the QED coupling α , two types of diagrams contribute to the QED processes. The first type consists of the diagrams shown in Fig. 1 (plus two others in which the directions of the arrows on the heavy-quark lines are reversed), but with the gluon replaced by a photon. The second type consists of diagrams in which a photon fragments into a J/ψ . One of these diagrams is shown in Fig. 2. (There is an additional diagram in which the directions of the arrows on the heavy-quark line on the η_c side are reversed.)

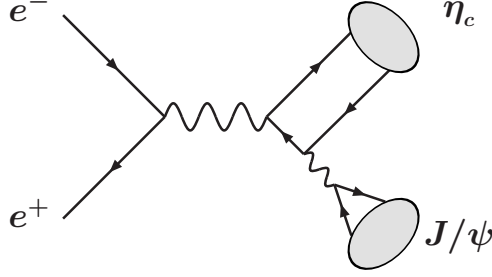


FIG. 2: Feynman diagram for the process $e^+e^- \rightarrow J/\psi + \eta_c$ in which a photon fragments into a J/ψ . There is an additional diagram that can be obtained by reversing the directions of the arrows on the heavy-quark line on the η_c side.

A. Kinematics

The Q and \bar{Q} that evolve into the charmonium H_i with momentum P_i have momenta p_i and \bar{p}_i , where $i = 1$ denotes the J/ψ and $i = 2$ denotes the η_c . The $Q(p_1)\bar{Q}(\bar{p}_1)$ pair is in a spin-triplet S -wave state and the $Q(p_2)\bar{Q}(\bar{p}_2)$ pair is in a spin-singlet S -wave state. The four-momenta of the Q and \bar{Q} in the i -th pair are expressed in terms of the total momentum P_i and the relative momentum q_i :

$$p_i = \frac{1}{2}P_i + q_i, \quad (4a)$$

$$\bar{p}_i = \frac{1}{2}P_i - q_i. \quad (4b)$$

P_i and q_i are chosen to be orthogonal: $P_i \cdot q_i = 0$. In the rest frame of the i -th $Q\bar{Q}$ pair, the explicit components of the momenta listed above are $P_i = [2E(q_i), \mathbf{0}]$, $q_i = (0, \mathbf{q}_i)$, $p_i = [E(q_i), \mathbf{q}_i]$, and $\bar{p}_i = [E(q_i), -\mathbf{q}_i]$, respectively, where $E(q_i) = \sqrt{m_c^2 + \mathbf{q}_i^2}$ is the energy of the Q or the \bar{Q} in the $Q\bar{Q}$ rest frame.

B. Spin and color projectors

A production amplitude of a $Q(p_i)\bar{Q}(\bar{p}_i)$ pair can be expressed in the form

$$\bar{u}(p_i)\mathcal{A}v(\bar{p}_i) = \text{Tr}[\mathcal{A}v(\bar{p}_i)\bar{u}(p_i)], \quad (5)$$

where \mathcal{A} is a matrix that acts on spinors with both Dirac and color indices. The amplitude in Eq. (5) can be projected into a particular spin and color channel by replacing $v(\bar{p}_i)\bar{u}(p_i)$

with a projection matrix. The color projector π_1 onto a color-singlet state is

$$\pi_1 = \frac{1}{\sqrt{N_c}} \mathbb{1}, \quad (6)$$

where $\mathbb{1}$ is the 3×3 unit matrix of the fundamental representation of $SU(3)$. The color-singlet projector (6) is normalized so that $\text{Tr}[\pi_1 \pi_1^\dagger] = 1$. The projector of the pair $Q(p_1)\bar{Q}(\bar{p}_1)$ onto a spin-triplet state with helicity λ and the projector of the pair $Q(p_2)\bar{Q}(\bar{p}_2)$ onto a spin-singlet state are denoted by $\Pi_3(p_1, \bar{p}_1, \lambda)$ and $\Pi_1(p_2, \bar{p}_2)$, respectively. The projectors, valid to all orders in \mathbf{q}_i , are given in Ref. [12]:

$$\Pi_3(p_1, \bar{p}_1, \lambda) = -\frac{1}{4\sqrt{2}E(q_1)[E(q_1) + m_c]} (\not{\vec{p}}_1 - m_c) \not{\epsilon}^*(\lambda) [\not{p}_1 + 2E(q_1)] (\not{p}_1 + m_c), \quad (7a)$$

$$\Pi_1(p_2, \bar{p}_2) = \frac{1}{4\sqrt{2}E(q_2)[E(q_2) + m_c]} (\not{\vec{p}}_2 - m_c) \gamma^5 [\not{p}_2 + 2E(q_2)] (\not{p}_2 + m_c), \quad (7b)$$

where the spin-polarization vector $\epsilon^*(\lambda)$ satisfies $P_1 \cdot \epsilon^*(\lambda) = 0$. The spin projectors in Eq. (7) are normalized so that

$$\text{Tr}[\Pi_3(p_1, \bar{p}_1, \lambda) \Pi_3^\dagger(p_1, \bar{p}_1, \lambda)] = 4p_1^0 \bar{p}_1^0, \quad (8a)$$

$$\text{Tr}[\Pi_1(p_2, \bar{p}_2) \Pi_1^\dagger(p_2, \bar{p}_2)] = 4p_2^0 \bar{p}_2^0. \quad (8b)$$

Since we are considering an exclusive process, in which no hadrons are present other than the J/ψ and the η_c , we consider only the states of the $Q\bar{Q}$ pairs that have the same quantum numbers as the J/ψ and the η_c . That is, the pair $Q(p_1)\bar{Q}(\bar{p}_1)$ must be in a color-singlet, spin-triplet S -wave state, as is the J/ψ , and the pair $Q(p_2)\bar{Q}(\bar{p}_2)$ must be in a color-singlet, spin-singlet S -wave state, as is the η_c .

The spin projectors in Eq. (7) can be simplified as follows:

$$\Pi_3(p_1, \bar{p}_1, \lambda) = -\frac{1}{2\sqrt{2}E(q_1)} (\not{\vec{p}}_1 - m_c) \left(\not{\epsilon}^*(\lambda) - \frac{(p_1 - \bar{p}_1) \cdot \epsilon^*(\lambda)}{2[E(q_1) + m_c]} \right) (\not{p}_1 + m_c), \quad (9a)$$

$$\Pi_1(p_2, \bar{p}_2) = \frac{1}{2\sqrt{2}E(q_2)} (\not{\vec{p}}_2 - m_c) \gamma^5 (\not{p}_2 + m_c). \quad (9b)$$

The spin projectors in Eq. (9) are also valid to all orders in \mathbf{q}_i .

In addition, we provide the following formulas, valid to all order in \mathbf{q}_i , that are useful in

this calculation:

$$\gamma_\alpha \Pi_3(p_1, \bar{p}_1, \lambda) \gamma^\alpha = \frac{1}{\sqrt{2}E(q_1)} \left[\not{p}_1 \not{\epsilon}^*(\lambda) \not{\bar{p}}_1 - m_c^2 \not{\epsilon}^*(\lambda) + (p_1 - \bar{p}_1) \cdot \epsilon^*(\lambda) \right. \\ \left. \times \left(2E(q_1) + \frac{m_c(\not{p}_1 - \not{\bar{p}}_1)}{2[E(q_1) + m_c]} \right) \right], \quad (10a)$$

$$\gamma_\alpha \Pi_1(p_2, \bar{p}_2) \gamma^\alpha = \frac{1}{\sqrt{2}} \gamma_5 \left[4E(q_2) - \frac{m_c}{E(q_2)} \not{p}_2 \right]. \quad (10b)$$

C. Projections of the four-quark states

From the full QCD amplitude for $\gamma^* \rightarrow Q(p_1)\bar{Q}(\bar{p}_1)Q(p_2)\bar{Q}(\bar{p}_2)$, one can project out the amplitude for $\gamma^* \rightarrow Q\bar{Q}(P_1, q_1, \lambda) + Q\bar{Q}(P_2, q_2)$, where the first pair is in a color-singlet, spin-triplet state with helicity λ and the second pair is in a color-singlet, spin-singlet state. Applying the spin-projection to both $Q\bar{Q}$ pairs simultaneously, one obtains

$$\mathcal{A}_Q^\mu(P_1, q_1, \lambda; P_2, q_2) = \text{Tr} \{ \mathcal{A}^\mu[\gamma^* \rightarrow Q(p_1)\bar{Q}(\bar{p}_1)Q(p_2)\bar{Q}(\bar{p}_2)] [\Pi_3(p_1, \bar{p}_1, \lambda) \otimes \pi_1] \otimes [\Pi_1(p_2, \bar{p}_2) \otimes \pi_1] \}, \quad (11)$$

where $\mathcal{A}^\mu[\gamma^* \rightarrow Q(p_1)\bar{Q}(\bar{p}_1)Q(p_2)\bar{Q}(\bar{p}_2)]$ is the full QCD amplitude for $\gamma^* \rightarrow Q(p_1)\bar{Q}(\bar{p}_1)Q(p_2)\bar{Q}(\bar{p}_2)$, μ is the vector index of the virtual photon, and $\mathcal{A}_Q^\mu(P_1, q_1, \lambda; P_2, q_2)$ is the amplitude for $\gamma^* \rightarrow Q\bar{Q}(P_1, q_1, \lambda) + Q\bar{Q}(P_2, q_2)$.

In the amplitude (11), the $Q\bar{Q}$ pairs are not necessarily in S -wave orbital-angular-momentum states. One can project out the S -wave amplitude by averaging, for each $Q\bar{Q}$ pair, over the direction of the relative momentum q_i in the $Q\bar{Q}(P_i)$ rest frame. The amplitude for $\gamma^* \rightarrow Q\bar{Q}(^3S_1, P_1, \lambda) + Q\bar{Q}(^1S_0, P_2)$ is

$$\mathcal{A}_Q^\mu(^3S_1, P_1, \lambda; ^1S_0, P_2) = \overline{\mathcal{A}_Q^\mu(P_1, q_1, \lambda; P_2, q_2)}, \quad (12)$$

where the bar on the right side of Eq. (12) is the average over the angles of both q_1 and q_2 in the P_1 and P_2 rest frames, respectively:

$$\overline{\mathcal{A}_Q^\mu(P_1, q_1, \lambda; P_2, q_2)} = \int \frac{d\Omega_1 d\Omega_2}{(4\pi)^2} \mathcal{A}_Q^\mu(P_1, q_1, \lambda; P_2, q_2). \quad (13)$$

$d\Omega_i$ is the solid-angle element of q_i , defined in the P_i rest frame. Once we have averaged over angles, the \mathbf{q}_i dependence in the amplitude (12) reduces a dependence only on \mathbf{q}_1^2 and \mathbf{q}_2^2 . Note that P_i depends on \mathbf{q}_i^2 implicitly: $P_i^2 = 4(m_c^2 + \mathbf{q}_i^2)$.

IV. NRQCD EXPANSION OF THE AMPLITUDE AND MATCHING

The NRQCD expansion of Eq. (3) in terms of the vacuum-to- J/ψ and vacuum-to- η_c matrix elements is

$$\mathcal{A}^\mu[J/\psi(\lambda) + \eta_c] = \sqrt{2m_1}\sqrt{2m_2} \sum_{m,n} d_{mn}^\mu \langle J/\psi(\lambda) | \mathcal{O}_m | 0 \rangle \langle \eta_c | \mathcal{O}_n | 0 \rangle, \quad (14)$$

where the d_{mn}^μ are short-distance coefficients and the \mathcal{O}_m and the \mathcal{O}_n are NRQCD operators. The quantities m_1 and m_2 represent the J/ψ and η_c masses, respectively. However, as we shall discuss later, these quantities are not necessarily equal to the physical meson masses, but may instead be expressed as functions of the heavy-quark masses via the nonrelativistic expansion of NRQCD. The factor $\sqrt{2m_1}\sqrt{2m_2}$ appears on the right side of Eq. (14) because we use relativistic normalization for the meson states in $\mathcal{A}^\mu[J/\psi(\lambda) + \eta_c]$, but we use conventional nonrelativistic normalization for the NRQCD matrix elements on the right side of Eq. (14).

Now we approximate the formula (14) by retaining only those operator matrix elements that connect the vacuum to the color-singlet $Q\bar{Q}$ Fock states of the quarkonia. Then, we have

$$\begin{aligned} \mathcal{A}^\mu[J/\psi(\lambda) + \eta_c] = \sqrt{2m_1}\sqrt{2m_2} \sum_{m=0}^{\infty} \sum_{n=0}^{\infty} c_{mn}^\mu(\lambda) \langle J/\psi(\lambda) | \psi^\dagger(-\frac{i}{2}\overleftrightarrow{\mathbf{D}})^{2m} \boldsymbol{\sigma} \cdot \boldsymbol{\epsilon}(\lambda) \chi | 0 \rangle \\ \times \langle \eta_c | \psi^\dagger(-\frac{i}{2}\overleftrightarrow{\mathbf{D}})^{2n} \chi | 0 \rangle, \end{aligned} \quad (15)$$

where the short-distance coefficients $c_{mn}^\mu(\lambda)$ are a subset of the short-distance coefficients d_{mn}^μ . ψ^\dagger and χ are two-component Pauli spinors that create a heavy quark and a heavy antiquark, respectively, σ^i is a Pauli matrix, and $\overleftrightarrow{\mathbf{D}}$ is the spatial part of the covariant derivative acting to the left and right anti-symmetrically. Note that there is no sum over λ on the right side of Eq. (15). All of the three-vector quantities in the NRQCD matrix elements for the H_i are defined in the P_i rest frame. We will clarify below the meaning of the approximation that we have taken to arrive at Eq. (15).

The short-distance coefficient $c_{mn}^\mu(\lambda)$ can be obtained from the full QCD amplitude

$\mathcal{A}_Q^\mu(^3S_1, P_1, \lambda; ^1S_0, P_2)$ in Eq. (12). The NRQCD expansion of the full QCD amplitude is

$$\begin{aligned}\mathcal{A}_Q^\mu(^3S_1, P_1, \lambda; ^1S_0, P_2) &= \sum_{m=0}^{\infty} \sum_{n=0}^{\infty} c_{mn}^\mu(\lambda) \langle Q\bar{Q}(^3S_1, \lambda) | \psi^\dagger (-\frac{i}{2} \overleftrightarrow{\mathbf{D}})^{2m} \boldsymbol{\sigma} \cdot \boldsymbol{\epsilon}(\lambda) \chi | 0 \rangle \\ &\quad \times \langle Q\bar{Q}(^1S_0) | \psi^\dagger (-\frac{i}{2} \overleftrightarrow{\mathbf{D}})^{2n} \chi | 0 \rangle \\ &= 8N_c E(q_1) E(q_2) \sum_{m=0}^{\infty} \sum_{n=0}^{\infty} c_{mn}^\mu(\lambda) \mathbf{q}_1^{2m} \mathbf{q}_2^{2n}.\end{aligned}\quad (16)$$

In Eq. (16), we use relativistic normalization for the Q and \bar{Q} states in the computation of $\mathcal{A}_Q^\mu(^3S_1, P_1, \lambda; ^1S_0, P_2)$ and in the computation of the NRQCD matrix elements. Consequently, a factor $4E(q_1)E(q_2)$ appears in the second equality of Eq. (16). An additional factor $2N_c$ arises from the spin and color factors of the NRQCD matrix elements. From Eq. (16), it is straightforward to calculate the short-distance coefficients $c_{mn}^\mu(\lambda)$:

$$c_{mn}^\mu(\lambda) = \frac{1}{m! n!} \frac{\partial^m}{\partial \mathbf{q}_1^{2m}} \frac{\partial^n}{\partial \mathbf{q}_2^{2n}} \left[\frac{\mathcal{A}_Q^\mu(^3S_1, P_1, \lambda; ^1S_0, P_2)}{8N_c E(q_1) E(q_2)} \right]_{\mathbf{q}_1^2 = \mathbf{q}_2^2 = 0}. \quad (17)$$

Substituting the short-distance coefficients (17) into Eq. (15), one finds that

$$\begin{aligned}\mathcal{A}^\mu[J/\psi(\lambda) + \eta_c] &= \sqrt{2m_1} \sqrt{2m_2} \langle J/\psi(\lambda) | \psi^\dagger \boldsymbol{\sigma} \cdot \boldsymbol{\epsilon}(\lambda) \chi | 0 \rangle \langle \eta_c | \psi^\dagger \chi | 0 \rangle \\ &\quad \times \sum_{m=0}^{\infty} \sum_{n=0}^{\infty} c_{mn}^\mu(\lambda) \langle \mathbf{q}^{2m} \rangle_{J/\psi} \langle \mathbf{q}^{2n} \rangle_{\eta_c} \\ &= \frac{\sqrt{2m_1} \sqrt{2m_2}}{2N_c} \langle J/\psi(\lambda) | \psi^\dagger \boldsymbol{\sigma} \cdot \boldsymbol{\epsilon}(\lambda) \chi | 0 \rangle \langle \eta_c | \psi^\dagger \chi | 0 \rangle \sum_{m=0}^{\infty} \sum_{n=0}^{\infty} \frac{\langle \mathbf{q}^{2m} \rangle_{J/\psi} \langle \mathbf{q}^{2n} \rangle_{\eta_c}}{m! n!} \\ &\quad \times \frac{\partial^m}{\partial \mathbf{q}_1^{2m}} \frac{\partial^n}{\partial \mathbf{q}_2^{2n}} \left[\frac{\mathcal{A}_Q^\mu(^3S_1, P_1, \lambda; ^1S_0, P_2)}{4E(q_1)E(q_2)} \right]_{\mathbf{q}_1^2 = \mathbf{q}_2^2 = 0}.\end{aligned}\quad (18)$$

Here, the quantities $\langle \mathbf{q}^{2m} \rangle_H$ are ratios of NRQCD matrix elements:

$$\langle \mathbf{q}^{2m} \rangle_{J/\psi} = \frac{\langle J/\psi(\lambda) | \psi^\dagger (-\frac{i}{2} \overleftrightarrow{\mathbf{D}})^{2m} \boldsymbol{\sigma} \cdot \boldsymbol{\epsilon}(\lambda) \chi | 0 \rangle}{\langle J/\psi(\lambda) | \psi^\dagger \boldsymbol{\sigma} \cdot \boldsymbol{\epsilon}(\lambda) \chi | 0 \rangle}, \quad (19a)$$

$$\langle \mathbf{q}^{2n} \rangle_{\eta_c} = \frac{\langle \eta_c | \psi^\dagger (-\frac{i}{2} \overleftrightarrow{\mathbf{D}})^{2n} \chi | 0 \rangle}{\langle \eta_c | \psi^\dagger \chi | 0 \rangle}. \quad (19b)$$

We note that $\langle J/\psi(\lambda) | \psi^\dagger \boldsymbol{\sigma} \cdot \boldsymbol{\epsilon}(\lambda) \chi | 0 \rangle$ and $\langle \mathbf{q}^{2m} \rangle_{J/\psi}$ are independent of the J/ψ helicity λ , and there are no sums over λ in these quantities.

Now we can clarify the meaning of the approximation that was taken to arrive at Eq. (15) and, consequently, to arrive at Eq. (18). Suppose that we specialize to the Coulomb gauge. Then, we can drop the gauge fields in covariant derivatives in the matrix elements in Eq. (18),

making errors of relative order v^2 . The matrix elements are then proportional to derivatives of the Coulomb-gauge color-singlet $Q\bar{Q}$ quarkonium wave function at the origin [2]. That is, $\langle \mathbf{q}^{2n} \rangle$ is just the $2n$ -th moment of the momentum-space wave function with respect to the wave-function momentum (the relative momentum of the Q and \bar{Q}). Hence, Eq. (18) has the interpretation of the convolution of the short-distance amplitude with the momentum-space quarkonium wave functions, where the short-distance coefficients have been Taylor expanded with respect to the wave-function momenta. Therefore, we see that the approximate NRQCD expansion in Eqs. (15) and (18) includes all of the relativistic corrections that are contained in the color-singlet $Q\bar{Q}$ quarkonium wave function, up to the ultraviolet cutoff of the NRQCD matrix elements.²

V. RESUMMATION

In Ref. [8], a method was presented for resumming a class of relativistic corrections to the color-singlet S -wave amplitudes that appear in the production and decay of S -wave quarkonium states. The key to the resummation is an expression that relates the S -wave color-singlet matrix elements of higher orders in v to the matrix elements of relative orders v^0 and v^2 :

$$\langle \mathbf{q}^{2n} \rangle_H = \langle \mathbf{q}^2 \rangle_H^n. \quad (20)$$

The relation (20) is derived in the approximation in which the Q and \bar{Q} interact only through the leading spin-independent potential. Consequently, the relation (20) is accurate up to corrections of relative order v^2 .³

The amplitude (18) is a function of the ratios $\langle \mathbf{q}^{2m} \rangle_{J/\psi}$ and $\langle \mathbf{q}^{2n} \rangle_{\eta_c}$. Applying the relation (20) to Eq. (15), one obtains the resummed expression

$$\begin{aligned} \mathcal{A}^\mu[J/\psi(\lambda) + \eta_c] &= \frac{1}{2N_c} \langle J/\psi(\lambda) | \psi^\dagger \boldsymbol{\sigma} \cdot \boldsymbol{\epsilon}(\lambda) \chi | 0 \rangle \langle \eta_c | \psi^\dagger \chi | 0 \rangle \\ &\times \left[\frac{\sqrt{2m_1} \sqrt{2m_2}}{2E(q_1) 2E(q_2)} A_Q^\mu(^3S_1, P_1, \lambda; ^1S_0, P_2) \right]_{\mathbf{q}_1^2 = \langle \mathbf{q}^2 \rangle_{J/\psi}, \mathbf{q}_2^2 = \langle \mathbf{q}^2 \rangle_{\eta_c}}. \end{aligned} \quad (21)$$

² We note that, in the case of dimensionally regulated NRQCD matrix elements, pure power ultraviolet divergences in the matrix elements are set to zero. Hence, the effects of pure-power-divergent contributions are absent in the resummation.

³ The derivation involves specializing to the Coulomb gauge and replacing covariant derivatives in operators with ordinary derivatives. This approximation also introduces errors of relative order v^2 .

The expression (21) resums those relativistic corrections that are contained in the $Q\bar{Q}$ quarkonium wave function, using the leading-potential model for the wave function. We note that, because the relation (20) is accurate only up to corrections of relative order v^2 , the use of the resummed expression (21) generally does not improve the nominal accuracy over that which one would obtain by retaining only corrections through relative order v^2 in Eq. (15). The exception to this is the situation in which the short-distance coefficients c_{mn}^μ in Eq. (17) grow rapidly with m or n . Then the terms of nominally higher order in v in Eq. (15) can have numerical values that are comparable to or larger than the numerical value of the term of nominal order v^2 . In that situation, the resummed expression can give an improved estimate of the amplitude. The resummed expression may also give an indication of the rate of convergence of the v expansion. In any case, it is generally useful to include a well-defined set of higher-order contributions in a calculation whenever possible.

VI. CHOICE OF FRAME AND CO-ORDINATE SYSTEM

In calculating $\mathcal{A}_Q^\mu(^3S_1, P_1, \lambda; ^1S_0, P_2)$, it is convenient to specialize to the e^+e^- CM frame, to choose a particular coordinate system, and to choose a particular convention for the polarization vectors of the $Q\bar{Q}_1(^3S_1)$ states for the various helicities. We make these choices as follows:

$$k_1 = \frac{\sqrt{s}}{2}(1, +\sin\theta, 0, +\cos\theta), \quad (22a)$$

$$k_2 = \frac{\sqrt{s}}{2}(1, -\sin\theta, 0, -\cos\theta), \quad (22b)$$

$$P_1^* = (E_1, 0, 0, +P_{\text{CM}}), \quad (22c)$$

$$P_2^* = (E_2, 0, 0, -P_{\text{CM}}), \quad (22d)$$

$$\epsilon^*(0) = \frac{1}{\sqrt{E_1^2 - P_{\text{CM}}^2}}(P_{\text{CM}}, 0, 0, E_1), \quad (22e)$$

$$\epsilon^*(\pm) = \mp \frac{1}{\sqrt{2}}(0, 1, \mp i, 0). \quad (22f)$$

Here, the angle θ is the scattering angle, four-vectors are written as $v = (v^0, v^1, v^2, v^3)$, and

$$P_{\text{CM}} = \frac{\lambda^{1/2}(s, \tilde{m}_1^2, \tilde{m}_2^2)}{2\sqrt{s}}, \quad (23a)$$

$$E_i = \sqrt{P_{\text{CM}}^2 + \tilde{m}_i^2}, \quad (23b)$$

where $\lambda(x, y, z) = x^2 + y^2 + z^2 - 2(xy + yz + zx)$. We have used the notation P_i^* to distinguish the particular values of these quantities in the e^+e^- CM frame from the values in the quarkonium rest frame (Sec. III A). As with the quantities m_1 and m_2 in Eq. (14), \tilde{m}_1 and \tilde{m}_2 represent the J/ψ and η_c masses, respectively. We will specify below how these are chosen for various parts of the calculation.

Now let us write expressions for the relative momenta q_1 and q_2 in the e^+e^- CM frame. In the quarkonium rest frame, q_i is given by

$$q_i = |\mathbf{q}_i|(0, \sin \theta_i \cos \phi_i, \sin \theta_i \sin \phi_i, \cos \theta_i), \quad (24)$$

where θ_i and ϕ_i are the polar and azimuthal angles of q_i . Boosting Eq. (24) from the P_i rest frame to the e^+e^- CM frame, one obtains

$$q_1^* = |\mathbf{q}_1|(+\gamma_1\beta_1 \cos \theta_1, \sin \theta_1 \cos \phi_1, \sin \theta_1 \sin \phi_1, \gamma_1 \cos \theta_1), \quad (25a)$$

$$q_2^* = |\mathbf{q}_2|(-\gamma_2\beta_2 \cos \theta_2, \sin \theta_2 \cos \phi_2, \sin \theta_2 \sin \phi_2, \gamma_2 \cos \theta_2), \quad (25b)$$

where

$$\gamma_i = E_i / \sqrt{E_i^2 - P_{\text{CM}}^2}, \quad (26a)$$

$$\gamma_i\beta_i = P_{\text{CM}} / \sqrt{E_i^2 - P_{\text{CM}}^2}. \quad (26b)$$

Note that $|\mathbf{q}_i| = \sqrt{-q_i^2}$ is the magnitude of the three-vector, not in the e^+e^- CM frame, but in the P_i rest frame.

It follows from Eq. (23) and the analogue of Eq. (3) for $\mathcal{A}_Q^\mu(^3S_1, P_1, \lambda; ^1S_0, P_2)$ that

$$\mathcal{A}_Q^\mu(^3S_1, P_1, 0; ^1S_0, P_2) = 0, \quad (27a)$$

$$\mathcal{A}_Q^\mu(^3S_1, P_1, \pm; ^1S_0, P_2) = \pm A_Q P_{\text{CM}} \sqrt{s} \epsilon^{*\mu}(\pm). \quad (27b)$$

It is efficient to determine A_Q by carrying out the computation of the amplitude $\mathcal{A}_Q^\mu(^3S_1, P_1, \lambda; ^1S_0, P_2)$ for one value of μ and one value of λ such that $\epsilon^{*\mu}(\lambda)$ is nonzero.

VII. CROSS SECTION

Making use of Eq. (3) and the explicit choices of helicity states in Eq. (22), we find that

$$\mathcal{A}^\mu[J/\psi(0) + \eta_c] = 0, \quad (28a)$$

$$\mathcal{A}^\mu[J/\psi(\pm) + \eta_c] = \pm A P_{\text{CM}} \sqrt{s} \epsilon^{*\mu}(\pm). \quad (28b)$$

Comparing Eq. (28) with Eq. (27) and making use of the resummed NRQCD expansion in Eq. (21), we see that

$$A = \frac{1}{2N_c} \langle J/\psi(\lambda) | \psi^\dagger \boldsymbol{\sigma} \cdot \boldsymbol{\epsilon}(\lambda) \chi | 0 \rangle \langle \eta_c | \psi^\dagger \chi | 0 \rangle \left[\frac{\sqrt{2m_1} \sqrt{2m_2}}{2E(q_1) 2E(q_2)} A_Q \right] \Big|_{\mathbf{q}_1^2 = \langle \mathbf{q}^2 \rangle_{J/\psi}, \mathbf{q}_2^2 = \langle \mathbf{q}^2 \rangle_{\eta_c}}. \quad (29)$$

$\mathcal{M}(\lambda)$, the S -matrix element for the process $e^+e^- \rightarrow J/\psi + \eta_c$, is defined in Eq. (1). By making use of Eqs. (3) and (28), one can evaluate $\mathcal{M}(\lambda)$:

$$\mathcal{M}(0) = 0, \quad (30a)$$

$$\mathcal{M}(\pm) = \pm A P_{\text{CM}} \sqrt{s} L \cdot \epsilon^*(\pm). \quad (30b)$$

The squared helicity amplitudes, summed over the spin states $s^+ = \pm 1/2$ and $s^- = \pm 1/2$ of the e^+ and e^- , respectively, can be obtained by using Eqs. (30) and (22):

$$\sum_{s^\pm = \pm 1/2} |L \cdot \epsilon^*(\pm)|^2 = \frac{e_c^2 e^4}{s^2} \text{Tr}[k_1 \not{\epsilon}(\pm) k_2 \not{\epsilon}^*(\pm)] = \frac{e_c^2 e^4}{s} (1 + \cos^2 \theta), \quad (31)$$

which lead to

$$\sum_{s^\pm = \pm 1/2} |\mathcal{M}(0)|^2 = 0, \quad (32a)$$

$$\sum_{s^\pm = \pm 1/2} |\mathcal{M}(\pm)|^2 = e_c^2 e^4 |A|^2 P_{\text{CM}}^2 (1 + \cos^2 \theta). \quad (32b)$$

Averaging the squared helicity amplitude (32) over the lepton spins, dividing by the flux $2s$, and integrating over the two-body phase space, we obtain the total cross section for $e^+e^- \rightarrow J/\psi + \eta_c$:

$$\begin{aligned} \sigma[e^+e^- \rightarrow J/\psi + \eta_c] &= \frac{1}{2s} \times \frac{1}{4} \times \Phi_2 \int_{-1}^1 \frac{d \cos \theta}{2} \sum_{\lambda=\pm} \sum_{s^\pm = \pm 1/2} |\mathcal{M}(\lambda)|^2 \\ &= \frac{16\pi^2}{3s} e_c^2 \alpha^2 |A|^2 P_{\text{CM}}^2 \Phi_2 \\ &= \frac{4\pi^2}{3N_c^2 s} e_c^2 \alpha^2 P_{\text{CM}}^2 \Phi_2 \langle \mathcal{O}_1 \rangle_{J/\psi} \langle \mathcal{O}_1 \rangle_{\eta_c} \\ &\quad \times \left[\frac{2m_1 2m_2}{4E^2(q_1) 4E^2(q_2)} |A_Q|^2 \right] \Big|_{\mathbf{q}_1^2 = \langle \mathbf{q}^2 \rangle_{J/\psi}, \mathbf{q}_2^2 = \langle \mathbf{q}^2 \rangle_{\eta_c}}, \end{aligned} \quad (33)$$

where

$$\langle \mathcal{O}_1 \rangle_{J/\psi} = |\langle J/\psi(\lambda) | \psi^\dagger \boldsymbol{\sigma} \cdot \boldsymbol{\epsilon}(\lambda) \chi | 0 \rangle|^2, \quad (34a)$$

$$\langle \mathcal{O}_1 \rangle_{\eta_c} = |\langle \eta_c | \psi^\dagger \chi | 0 \rangle|^2, \quad (34b)$$

and Φ_2 is the two-body phase space

$$\Phi_2 = \frac{1}{8\pi s} \lambda^{1/2}(s, m_{J/\psi}^2, m_{\eta_c}^2). \quad (35)$$

Note that we use the physical masses for the J/ψ and the η_c in the phase space (35).

VIII. VMD TREATMENT OF THE PHOTON-FRAGMENTATION AMPLITUDE

In the part of the amplitude that comes from the photon-fragmentation diagrams of the type in Fig. 2, we can reduce the theoretical uncertainty by making use of the VMD method to calculate the fragmentation of the γ^* into J/ψ (Ref. [13]). In Ref. [13], the process $\gamma^* \rightarrow J/\psi$ has been calculated using the VMD method. Using Eq. (3) of Ref. [13], we find that the $\gamma^* \rightarrow J/\psi$ coupling is

$$g_{J/\psi} = \left(\frac{3m_{J/\psi}^3}{4\pi\alpha^2} \Gamma[J/\psi \rightarrow \ell^+ \ell^-] \right)^{1/2}. \quad (36)$$

In order to implement the VMD calculation we must make the following substitutions in the NRQCD calculation of the photon-fragmentation diagrams:

$$e_c \sqrt{2m_1 \langle \mathcal{O}_1 \rangle_{J/\psi}} \rightarrow g_{J/\psi}, \quad (37a)$$

$$\frac{\text{Tr}\{(\gamma_\mu \otimes \mathbb{1})[\Pi_3(p_1, \bar{p}_1, \lambda) \otimes \pi_1]\}}{\sqrt{2N_c} 2E(q_1)} \rightarrow \epsilon_\mu^*(\lambda), \quad (37b)$$

where $g_{J/\psi}$ is defined in Eq. (36).

IX. CHOICE OF THE QUARKONIUM MASSES

We now specify our choices of the quarkonium masses in our computation. In computing diagrams involving on-shell quarks, such as those in Fig. 1, it is generally necessary, in order to maintain gauge invariance, to choose the quarkonium masses so as to respect the on-shell condition. Hence, we generally must choose $\tilde{m}_i = 2E(q_i) = 2\sqrt{m_c^2 + \mathbf{q}_i^2}$ in Eq. (23) in working out the kinematics.

An exception to this is in the computation of the photon-fragmentation diagrams of the type in Fig. 2. In this case, if we make use of the VMD method for calculating the amplitude,

we can maintain gauge invariance even if we take \tilde{m}_1 to be $m_{J/\psi}$, the physical J/ψ mass. We still must choose $\tilde{m}_2 = 2E(q_2)$ for the η_c mass, however. Since one generally reduces theoretical uncertainties by eliminating $2m_c$ in favor of $m_{J/\psi}$, we choose $\tilde{m}_1 = m_{J/\psi}$ in the VMD calculation of the photon-fragmentation diagrams.

The factor $\sqrt{2m_1}\sqrt{2m_2}$ in Eq. (21) arises from the relativistic normalizations of the states. In this case, we choose $m_i = 2E(q_i)$. It turns out that this choice leads to a near cancellation of the dependence on m_c in the amplitude at leading order in v (Ref. [3]). Thus, this choice reduces the theoretical uncertainties that arise from the uncertainty in m_c .

Finally, as we have already noted, we use the physical quarkonium masses in computing the phase space in Eq. (35). At first sight, this choice might appear to be inconsistent with the choice $m_i = 2E(q_i)$ in Eq. (21), since the factors m_i in Eq. (21) arise from the normalizations of the states, which also enter into the phase space. The choices that we have made amount to multiplying the amplitude by the factors $\sqrt{2E(q_1)/m_{J/\psi}}$ and $\sqrt{2E(q_2)/m_{\eta_c}}$. At the level of precision in the v to which we work, these factors are equivalent to unity.

X. INTERFERENCE WITH THE NLO AMPLITUDE

As we have mentioned, the corrections to $\sigma[e^+e^- \rightarrow J/\psi + \eta_c]$ at NLO in α_s have been calculated in Ref. [7]. Because the amplitude for the relativistic corrections has the same phase as the amplitude at leading order in v , we can infer, from the results of Ref. [7], the contribution to the cross section of the interference between the amplitude at NLO in α_s and the amplitude for the relativistic corrections.

First, let us define some notation. When we discuss cross sections σ and reduced hadronic amplitudes A [Eq. (3)], a subscript 0 indicates that the quantity is computed at leading order in v , a subscript v indicates that the quantity is resummed to all orders in v , a subscript NLO on A indicates the contribution to A at NLO in α_s , and a subscript NLO on σ indicates the sum of the contributions to σ through NLO in α_s . A superscript QCD indicates that only QCD contributions to the hadronic amplitude have been included. The absence of a superscript QCD indicates that both QCD and pure QED contributions to the hadronic

amplitude have been included. Using this notation, we have

$$\sigma_0 = \mathcal{N}|A_0|^2, \quad (38a)$$

$$\sigma_v = \mathcal{N}|A_v|^2, \quad (38b)$$

$$\sigma_0^{\text{QCD}} = \mathcal{N}|A_0^{\text{QCD}}|^2, \quad (38c)$$

$$\sigma_{0,\text{NLO}}^{\text{QCD}} = \mathcal{N}\left[|A_0^{\text{QCD}}|^2 + 2\text{Re}(A_0^{\text{QCD}}A_{0,\text{NLO}}^{*\text{QCD}})\right], \quad (38d)$$

where the normalization factor \mathcal{N} is that of Eq. (33) and is defined by

$$\mathcal{N} = \frac{16\pi^2}{3s}e_c^2\alpha^2P_{\text{CM}}^2\Phi_2, \quad (39)$$

with P_{CM} defined in Eq. (23) and Φ_2 defined in Eq. (35).

The quantity $\sigma_{0,\text{NLO}}^{\text{QCD}}$ is computed in Ref. [7]. On the other hand, we wish to compute the quantity

$$\sigma_{\text{tot}} = \mathcal{N}\left[|A_v|^2 + 2\text{Re}(A_vA_{0,\text{NLO}}^{*\text{QCD}})\right]. \quad (40)$$

Using the fact that A_v and A_0^{QCD} have the same phase, we can write

$$\begin{aligned} 2\text{Re}(A_vA_{0,\text{NLO}}^{*\text{QCD}}) &= \frac{A_v}{A_0^{\text{QCD}}} 2\text{Re}(A_0^{\text{QCD}}A_{0,\text{NLO}}^{*\text{QCD}}) \\ &= \frac{1}{\mathcal{N}}\sqrt{\sigma_v} \frac{\sigma_{0,\text{NLO}}^{\text{QCD}} - \sigma_0^{\text{QCD}}}{\sqrt{\sigma_0^{\text{QCD}}}}. \end{aligned} \quad (41)$$

Thus, σ_{tot} can be expressed in terms of σ_v , σ_0^{QCD} , and $\sigma_{0,\text{NLO}}^{\text{QCD}}$:

$$\sigma_{\text{tot}} = \sigma_v + \sqrt{\sigma_v} \frac{\sigma_{0,\text{NLO}}^{\text{QCD}} - \sigma_0^{\text{QCD}}}{\sqrt{\sigma_0^{\text{QCD}}}}. \quad (42)$$

XI. RESULTS

In this section, we present our numerical results.

We compute A_Q in Eq. (27) from the Feynman diagrams in Figs. 1 and 2, making use of the spin and color projectors, as described in Section III. We then carry out the projection onto the S -wave states by performing the integration over the angles of \mathbf{q}_1 and \mathbf{q}_2 numerically, as indicated in Eq. (13). We substitute A_Q into Eq. (29) to obtain A and substitute A into Eq. (33) to obtain the cross section σ_v , which includes the resummed relativistic corrections.

We compute the cross section at leading order in v , σ_0 , by setting $\mathbf{q}_1^2 = \mathbf{q}_2^2 = 0$ in the expressions for σ_v .

In carrying out this calculation, we make use of the matrix elements $\langle \mathcal{O}_1 \rangle_{J/\psi}$ and $\langle \mathcal{O}_1 \rangle_{\eta_c}$ and the ratios of matrix elements $\langle \mathbf{q}^2 \rangle_{J/\psi}$ and $\langle \mathbf{q}^2 \rangle_{\eta_c}$ from Tables I and III of Ref. [11]. In Ref. [11], various uncertainties were associated with these quantities. The uncertainties are correlated to varying degrees among the quantities. We recount the uncertainties here.

There are theoretical uncertainties in the values of $\langle \mathbf{q}^2 \rangle_{J/\psi}$ and $\langle \mathbf{q}^2 \rangle_{\eta_c}$ that arise from the fact that the leading-potential approximation that is used in Ref. [11] is accurate only up to corrections of relative order v^2 . These uncertainties are denoted by $\Delta \langle \mathbf{q}^2 \rangle_{J/\psi}$ and $\Delta \langle \mathbf{q}^2 \rangle_{\eta_c}$, respectively. There are uncertainties that arise from the scale uncertainties in α_s and from neglecting next-to-next-to-leading-order (NNLO) corrections to the J/ψ and η_c electromagnetic widths. These are denoted by $\Delta \text{NNLO}_{J/\psi}$ and $\Delta \text{NNLO}_{\eta_c}$, respectively. There are also uncertainties that are associated with the heavy-quark mass m_c , the string tension σ , and the uncertainties in the experimental measurements of $\Gamma[J/\psi \rightarrow e^+e^-]$ and $\Gamma[\eta_c \rightarrow \gamma\gamma]$. These uncertainties are denoted by Δm_c , $\Delta\sigma$, $\Delta\Gamma_{J/\psi}$, and $\Delta\Gamma_{\eta_c}$, respectively. Finally, there is an uncertainty that is associated with the use of the heavy-quark spin symmetry to combine the values of the η_c matrix elements that were obtained from $\Gamma[\eta_c \rightarrow \gamma\gamma]$ with those that were obtained from $\Gamma[J/\psi \rightarrow e^+e^-]$. It is denoted by Δv^2 .

The calculation requires some additional inputs. We take $\sqrt{s} = 10.58$ GeV. In order to maintain consistency with the calculation at NLO in α_s in Ref. [7], we take m_c to be the one-loop pole mass. The specific numerical value that we use is⁴

$$m_c = 1.4 \pm 0.2 \text{ GeV}. \quad (43)$$

This choice of numerical value corresponds to the one in Ref. [11], and so, in determining the uncertainties that arise from the uncertainty in m_c , we are able to make use of the dependences of the matrix elements and ratios of matrix elements on m_c that are computed

⁴ The most recent compilation of the Particle Data Group [14] suggests that the uncertainty in m_c may be a factor of two smaller than the uncertainty that we have used here. However, since it is not clear that the systematic errors are well understood in the various determinations that enter into that compilation, we make a conservative choice of error bars here.

in Ref. [11]. For the strong and electromagnetic couplings we take⁵

$$\alpha_s(10.58/4 \text{ GeV}) = 0.26, \quad (44a)$$

$$\alpha_s(10.58/2 \text{ GeV}) = 0.21, \quad (44b)$$

$$\alpha_s(10.58 \text{ GeV}) = 0.17, \quad (44c)$$

and

$$\alpha(10.58/4 \text{ GeV}) = (132.9)^{-1}, \quad (45a)$$

$$\alpha(10.58/2 \text{ GeV}) = (131.9)^{-1}, \quad (45b)$$

$$\alpha(10.58 \text{ GeV}) = (130.9)^{-1}, \quad (45c)$$

$$\alpha(m_{J/\psi}) = (132.6)^{-1}. \quad (45d)$$

We determine the central values of the scales for couplings from the momentum transfer at the relevant vertex: At c -quark-gluon vertices, we take the scale to be half the CM energy; at the photon-electron and non-fragmentation-photon- c -quark vertices, we take the scale to be the CM energy; at the fragmentation-photon- c -quark vertices, we take the scale to be the J/ψ mass. These choices are consistent with those in Ref. [11]. We also use $m_{J/\psi} = 3.096916 \text{ GeV}$ and $m_{\eta_c} = 2.9798 \text{ GeV}$ [14].

In computing the cross section σ_{tot} , which includes relativistic corrections, corrections of NLO in α_s , and the interference between them, we make use of Eq. (42). We compute the quantity $(\sigma_{0,\text{NLO}}^{\text{QCD}} - \sigma_0^{\text{QCD}})/\sqrt{\sigma_0^{\text{QCD}}}$ by making use of results [16] that have been provided by the authors of Ref. [7]. These results are shown in Table I. Here we have introduced an additional uncertainty $\Delta\mu$, which accounts for effects of the uncertainty in the renormalization scale in the NLO calculation. This uncertainty is determined by varying the renormalization scale by a factor of two above and below its central value of $10.58/2 \text{ GeV}$. In making use of the results from the authors of Ref. [7], we rescale the values of α_s , α , the matrix elements $\langle \mathcal{O}_1 \rangle_{J/\psi}$ and $\langle \mathcal{O}_1 \rangle_{\eta_c}$, and the phase space so that they conform to our choices. The rescaling is carried out as follows:

$$\frac{\sigma_{0,\text{NLO}}^{\text{QCD}} - \sigma_0^{\text{QCD}}}{\sqrt{\sigma_0^{\text{QCD}}}} = \sqrt{\rho} \times \frac{\sigma_{0,\text{NLO}}^{\text{ZGC}} - \sigma_0^{\text{ZGC}}}{\sqrt{\sigma_0^{\text{ZGC}}}}, \quad (46)$$

⁵ We compute α_s and α at each scale by making use of the code GLOBAL ANALYSIS OF PARTICLE PROPERTIES (GAPP) [15].

TABLE I: The cross sections in units of fb that were obtained by Zhang, Gao, and Chao [7, 16]. The first row below the headings contains the cross sections for central values of m_c and μ . Subsequent rows contain the cross sections for the plus and minus variations of m_c and μ with respect to their uncertainties. The strong coupling constant was taken to be $\alpha_s^{\text{ZGC}}(10.6/4 \text{ GeV}) = 0.273$, $\alpha_s^{\text{ZGC}}(10.6/2 \text{ GeV}) = 0.211$, and $\alpha_s^{\text{ZGC}}(10.6 \text{ GeV}) = 0.174$ (Ref. [16]).

case	σ_0^{ZGC}	$\sigma_{0,\text{NLO}}^{\text{ZGC}}$
central	5.8	12.6
$+\Delta Q_2 = +\Delta m_c$	4.8	9.7
$-\Delta Q_2 = -\Delta m_c$	6.7	15.7
$+\Delta Q_{10} = +\Delta \mu$	3.9	8.9
$-\Delta Q_{10} = -\Delta \mu$	9.6	19.6

where the superscript ZGC indicates the quantities from the authors of Ref. [7]. The scaling factor ρ is defined by

$$\rho = \left(\frac{\alpha = 1/130.9}{\alpha^{\text{ZGC}} = 1/137} \right)^2 \left(\frac{\alpha_s(\mu)}{\alpha_s^{\text{ZGC}}(\mu)} \right)^2 \frac{\langle \mathcal{O}_1 \rangle_{J/\psi} \langle \mathcal{O}_1 \rangle_{\eta_c}}{\left(\langle \mathcal{O}_1 \rangle_{J/\psi}^{\text{ZGC}} \right)^2} \frac{\Phi_2}{\Phi_2^{\text{ZGC}}}. \quad (47)$$

The values for Φ_2^{ZGC} and $\langle \mathcal{O}_1 \rangle_{1S}^{\text{ZGC}}$ are given by

$$\Phi_2^{\text{ZGC}} = \frac{1}{8\pi} \times \sqrt{1 - \left(\frac{4m_c}{\sqrt{s}} \right)^2}, \quad (48a)$$

$$\langle \mathcal{O}_1 \rangle_{1S}^{\text{ZGC}} = \frac{3}{2\pi} \times 0.978 \text{ GeV}^3 = 0.467 \text{ GeV}^3. \quad (48b)$$

Our numerical results are shown in Table II. The first row below the headings gives the central values of the matrix elements, ratios of matrix elements, and the cross sections. Subsequent rows contain the maximum and minimum values of each of these quantities that are obtained by varying the input parameters with respect to each of the uncertainties that we have described. The matrix elements and the ratios, as well as their variations with respect to each uncertainty, are taken from Tables I and III of Ref. [11]. The deviations from the central values, given in the same order as the rows in Table II, are as follows:

$$\sigma_0 = 6.4_{-0.1-0.5-0.1-1.1-0.2-1.1-0.3-0.4-0.7}^{+0.1+0.5+0.1+1.5+0.3+1.1+0.4+0.5+0.7} \text{ fb} = 6.4_{-1.9}^{+2.1} \text{ fb}, \quad (49a)$$

$$\sigma_v = 9.3_{-0.8-1.7-0.4-1.5-0.3-1.5-0.7-0.6-1.0}^{+0.7+2.5+0.4+2.0+0.4+1.5+0.7+0.7+1.0} \text{ fb} = 9.3_{-3.2}^{+4.0} \text{ fb}, \quad (49b)$$

$$\sigma_{\text{tot}} = 17.6_{-1.2-3.7-0.7-3.0-0.7-2.9-1.2-1.1-2.0}^{+1.2+5.3+0.7+3.9+0.7+2.9+1.2+1.4+1.9} \text{ fb} = 17.6_{-6.3}^{+7.8} \text{ fb}. \quad (49c)$$

TABLE II: The matrix elements $\langle \mathcal{O}_1 \rangle_{J/\psi}$ and $\langle \mathcal{O}_1 \rangle_{\eta_c}$ in units of GeV^3 , the ratios of matrix elements $\langle \mathbf{q}^2 \rangle_{J/\psi}$ and $\langle \mathbf{q}^2 \rangle_{\eta_c}$ in units of GeV^2 , and the cross sections σ_0 , σ_v , and σ_{tot} in units of fb. The first row below the headings contains central values for the matrix elements, the ratios, and the cross sections. Subsequent rows contain the maximum and minimum values of each of these quantities that are obtained by varying the input parameters with respect to each uncertainty. The last two rows contain the values that are obtained when the renormalization scale μ is multiplied or divided by a factor of two, as in the last two rows of Table I.

case	$\langle \mathcal{O}_1 \rangle_{J/\psi}$	$\langle \mathbf{q}^2 \rangle_{J/\psi}$	$\langle \mathcal{O}_1 \rangle_{\eta_c}$	$\langle \mathbf{q}^2 \rangle_{\eta_c}$	σ_0	σ_v	σ_{tot}
central	0.440	0.441	0.437	0.442	6.4	9.3	17.6
$+\Delta Q_1 = +\Delta \langle \mathbf{q}^2 \rangle_{J/\psi}$	0.450	0.573	0.438	0.511	6.6	10.0	18.7
$-\Delta Q_1 = -\Delta \langle \mathbf{q}^2 \rangle_{J/\psi}$	0.430	0.308	0.437	0.372	6.3	8.5	16.4
$+\Delta Q_2 = +\Delta m_c$	0.433	0.443	0.469	0.432	6.0	7.6	13.9
$-\Delta Q_2 = -\Delta m_c$	0.451	0.437	0.413	0.449	6.9	11.8	22.8
$+\Delta Q_3 = +\Delta \sigma$	0.443	0.482	0.444	0.482	6.6	9.7	18.3
$-\Delta Q_3 = -\Delta \sigma$	0.437	0.400	0.431	0.402	6.3	8.9	16.9
$+\Delta Q_4 = +\Delta \text{NNLO}_{J/\psi}$	0.504	0.419	0.473	0.429	7.9	11.3	21.5
$-\Delta Q_4 = -\Delta \text{NNLO}_{J/\psi}$	0.387	0.459	0.408	0.452	5.3	7.7	14.6
$+\Delta Q_5 = +\Delta \Gamma_{J/\psi}$	0.451	0.437	0.444	0.439	6.7	9.7	18.3
$-\Delta Q_5 = -\Delta \Gamma_{J/\psi}$	0.429	0.444	0.431	0.444	6.2	8.9	16.9
$+\Delta Q_6 = +\Delta v^2$	0.440	0.441	0.510	0.439	7.5	10.8	20.5
$-\Delta Q_6 = -\Delta v^2$	0.440	0.441	0.364	0.444	5.3	7.7	14.6
$+\Delta Q_7 = +\Delta \langle \mathbf{q}^2 \rangle_{\eta_c}$	0.440	0.441	0.461	0.505	6.8	10.0	18.8
$-\Delta Q_7 = -\Delta \langle \mathbf{q}^2 \rangle_{\eta_c}$	0.440	0.441	0.415	0.378	6.1	8.6	16.4
$+\Delta Q_8 = +\Delta \text{NNLO}_{\eta_c}$	0.440	0.441	0.474	0.430	7.0	10.0	19.0
$-\Delta Q_8 = -\Delta \text{NNLO}_{\eta_c}$	0.440	0.441	0.409	0.451	6.0	8.7	16.5
$+\Delta Q_9 = +\Delta \Gamma_{\eta_c}$	0.440	0.441	0.486	0.426	7.1	10.3	19.4
$-\Delta Q_9 = -\Delta \Gamma_{\eta_c}$	0.440	0.441	0.386	0.459	5.7	8.3	15.6
$+\Delta Q_{10} = +\Delta \mu$	0.440	0.441	0.437	0.442	4.4	6.3	12.3
$-\Delta Q_{10} = -\Delta \mu$	0.440	0.441	0.437	0.442	9.5	13.9	24.9

In the result for σ_{tot} above, we have not included the uncertainty $\Delta\mu$ that arises from varying the renormalization scale. That uncertainty is $^{+7.4}_{-5.3}$ fb. This is, perhaps, an overestimate of the uncertainty from uncalculated corrections of higher order in α_s and v^2 , since it assumes that our choice of renormalization scale may be wrong by as much as a factor of two. Alternatively, one could estimate the uncertainty that arises from uncalculated corrections in the following way. One could take for the uncertainty associated with uncalculated corrections of NNLO in α_s to be the quantity $\Delta\text{NNLO} = \alpha_s^2\sigma_{\text{tot}} \approx 0.77$ fb, and one could take for the uncertainty associated with uncalculated corrections of NLO in α_s and NLO in v^2 the quantity $\Delta\text{NLO-}v^2 = \alpha_s v^2\sigma_{\text{tot}} \approx 1.11$ fb. (Uncertainties of relative order v^4 are already included in $\Delta\langle\mathbf{q}^2\rangle_{J/\psi}$ and $\Delta\langle\mathbf{q}^2\rangle_{\eta_c}$.) If we add the uncertainty $\Delta\mu$ in quadrature with the other uncertainties, then we obtain

$$\sigma_{\text{tot}} = 17.6^{+10.8}_{-8.2} \text{ fb.} \quad (50)$$

On the other hand, if we add ΔNNLO and $\Delta\text{NLO-}v^2$ in quadrature with the other uncertainties, then we obtain

$$\sigma_{\text{tot}} = 17.6^{+7.9}_{-6.4} \text{ fb.} \quad (51)$$

In addition to the uncertainties that we have included in Eqs. (50) and (51), there are uncertainties that are associated with the NRQCD factorization formula. A rigorous proof of NRQCD factorization for $\sigma[e^+e^- \rightarrow J/\psi + \eta_c]$ does not exist. However, it seems likely, on the basis of existing work on proving NRQCD factorization for other production processes [17], that the corrections to the factorization formula are of order $m_H^2/(s/4) \approx 34\%$, where m_H is the mass of either of the heavy quarkonia.

The various contributions to σ_{tot} are as follows. The cross section at leading order in α_s and v , σ_0 , contributes about 6.4 fb, of which about 1.0 fb comes from the pure QED corrections. The direct relativistic corrections that are associated with the process $e^+e^- \rightarrow J/\psi + \eta_c$ contribute about 2.9 fb. The corrections of NLO in α_s contribute about 6.9 fb. The interference between the relativistic corrections and the corrections of NLO in α_s contributes about 1.4 fb.

We have examined our numerical calculation in the limits $\langle\mathbf{q}^2\rangle_{J/\psi} \rightarrow 0$ and $\langle\mathbf{q}^2\rangle_{\eta_c} \rightarrow 0$ and find that it agrees with the analytic results in Refs. [3] and [10] for the order- v^2 corrections to $\sigma[e^+e^- \rightarrow J/\psi + \eta_c]$.

The use of the VMD method, rather than the NRQCD method, in calculating the fragmentation amplitude in the pure QED contribution, has a small effect on the central value of the cross section. The use of the VMD method shifts the central value of σ_v down by about 3%.

The direct relativistic corrections to the process $e^+e^- \rightarrow J/\psi + \eta_c$ itself are modest in size. σ_v is about 45% larger than σ_0 , but σ_0 already contains an implicit relativistic correction factor of 0.96 that arises from the use of the hadron masses, rather than $2m_c$, in the phase space. Hence, the direct relativistic correction is about 40%. The order- v^2 relativistic corrections by themselves increase the cross section by about 45%. Thus, we see that the effects of resummation are not large, suggesting that the velocity expansion of NRQCD is converging well in this case.

As we have mentioned previously, the resummed result contains all of the corrections that are associated with the momentum-space $Q\bar{Q}$ quarkonium wave function in the leading-potential approximation, up to the ultraviolet cutoff of the NRQCD matrix elements. Hence, the modest size of the relativistic corrections supports the conclusion in Ref. [18] that the effects of the finite width of the momentum-space $Q\bar{Q}$ wave function are small, once one excludes contributions from the large-momentum tails of the wave function. Those contributions are included in the NRQCD formalism in the corrections of higher order in α_s .

XII. COMPARISON WITH PREVIOUS CALCULATIONS

Let us now compare our results with some of those from previous calculations.

As we have already mentioned, the contribution to $\sigma[e^+e^- \rightarrow J/\psi + \eta_c]$ at leading order in α_s and v was first calculated in Refs. [3] and [4]. There are some differences in these results, owing to different choices of input parameters and the inclusion of pure QED corrections in Ref. [3]. Let us focus on Ref. [3], since the calculation in that paper is closer to the present one in terms of input parameters and the treatment of pure QED corrections. The result in Ref. [3] is $\sigma[e^+e^- \rightarrow J/\psi + \eta_c] = 3.78 \pm 1.26$ fb. This result should be compared with our result for σ_0 , which is about 70% larger. This difference arises essentially because we have used the values for $\langle \mathcal{O}_1 \rangle_{J/\psi}$ and $\langle \mathcal{O}_1 \rangle_{\eta_c}$ from Ref. [11] (see Table II), while the authors of Ref. [3] have used $\langle \mathcal{O}_1 \rangle_{J/\psi} = \langle \mathcal{O}_1 \rangle_{\eta_c} = 0.335 \text{ GeV}^3$. This substantial difference in the values of the matrix elements arises largely from the inclusion of relativistic corrections

to the electromagnetic decay widths of the J/ψ and the η_c in analyses of Ref. [11]. The relativistic corrections increase the size of $\langle \mathcal{O}_1 \rangle_{J/\psi}$ by about 31% and increase the size of $\langle \mathcal{O}_1 \rangle_{\eta_c}$ by about 41% (Ref. [11]). The changes in the values of the matrix elements lead to a 71% change in the cross section. Other small differences in our calculation relative to that in Ref. [3] arise from using the VMD method to calculate the fragmentation contribution to the pure QED amplitude (about -8%), from the use of the physical masses for the J/ψ and the η_c in the phase space (about -4%), and from taking into account the effects of the running of α (about 10%). The error bar in the result of Ref. [3] takes into account only the uncertainty Δm_c . It is more than twice the size of the Δm_c error bar in σ_0 in our calculation. The error bar in our calculation is reduced because the Δm_c uncertainty in the matrix elements in Ref. [11] was reduced by replacing certain factors of $2m_c$ with $m_{J/\psi}$.

In Ref. [9], a result $\sigma_{\text{tot}} = 17.5 \pm 5.7$ fb is given. Our calculation contains a number of refinements in comparison with that of Ref. [9]. Among them are the use of the improved results for the matrix elements in Ref. [11], the use of the VMD method to calculate the fragmentation contribution to the pure QED amplitude, the inclusion of the effects of the running of α , and the precise calculation of the interference between the relativistic corrections and the corrections of NLO in α_s , rather than the use of an overall K factor to account for the corrections of NLO in α_s . The effects of these refinements cancel almost exactly in the central value for the cross section. The error bars in the result of Ref. [9] include only the uncertainties Δm_c , $\Delta \langle \mathbf{q}^2 \rangle_{J/\psi}$, and $\Delta \langle \mathbf{q}^2 \rangle_{\eta_c}$ and are, therefore, somewhat smaller than the error bars that we report here.

We can also compare our results with those of Ref. [10]. In that work, the quantities $\langle \mathcal{O}_1 \rangle_{J/\psi}$, $\langle \mathcal{O}_1 \rangle_{\eta_c}$, and $\langle \mathbf{q}^2 \rangle_{J/\psi} \langle \mathcal{O}_1 \rangle_{J/\psi} = \langle \mathbf{q}^2 \rangle_{\eta_c} \langle \mathcal{O}_1 \rangle_{\eta_c}$ were determined by comparing theoretical expressions for $\Gamma[J/\psi \rightarrow e^+e^-]$, $\Gamma[\eta_c \rightarrow \gamma\gamma]$, and $\Gamma[J/\psi \rightarrow \text{light hadrons}]$ with the experimental measurements of those widths. The resulting values are $\langle \mathcal{O}_1 \rangle_{J/\psi}^{\text{ZGC}} = 0.573 \text{ GeV}^3$, $\langle \mathcal{O}_1 \rangle_{\eta_c}^{\text{ZGC}} = 0.432 \text{ GeV}^3$, $\langle \mathbf{q}^2 \rangle_{J/\psi}^{\text{ZGC}} = 0.202 \text{ GeV}^2$, and $\langle \mathbf{q}^2 \rangle_{\eta_c}^{\text{ZGC}} = 0.268 \text{ GeV}^2$. The value of $\langle \mathcal{O}_1 \rangle_{J/\psi}$ is about 30% larger than the one that we employ, and the value of $\langle \mathcal{O}_1 \rangle_{\eta_c}$ is about 1% smaller. The values of $\langle \mathbf{q}^2 \rangle_{J/\psi}$ and $\langle \mathbf{q}^2 \rangle_{\eta_c}$ are smaller than the values that we use by about 54% and 39%, respectively, and are considerably smaller than expectations from the NRQCD velocity-scaling rules. As was discussed in Ref. [11], the smaller values of $\langle \mathbf{q}^2 \rangle_{J/\psi}$ and $\langle \mathbf{q}^2 \rangle_{\eta_c}$ arise in Ref. [10] because the theoretical expression for $\Gamma[J/\psi \rightarrow \text{light hadrons}]$ contains a very large relativistic correction. We regard this as an indication that the velocity-expansion

for that process is not under control.

The authors of Ref. [10] find that the relativistic corrections to $\sigma[e^+e^- \rightarrow J/\psi + \eta_c]$ enhance the cross section by about 26%. This is somewhat smaller than the enhancement that we find of about 45% (without resummation). The difference presumably arises from the use of smaller values of $\langle \mathbf{q}^2 \rangle_{J/\psi}$ and $\langle \mathbf{q}^2 \rangle_{\eta_c}$ in Ref. [10].

In Ref. [10], the central value for the total cross section is $\sigma_{\text{tot}}^{\text{ZGC}} = 20.04$ fb. This result does not include the pure QED contribution, the contribution from the interference between the corrections of NLO in α_s and the relativistic corrections, and the effects of resummation. The corresponding quantity in our calculation is 15.3 fb. Thus, we see that the result of Ref. [10] is 31% larger than ours. The main sources of this difference are the use of a larger value of $\langle \mathcal{O}_1 \rangle_{J/\psi}$, which would increase our cross section by about 30%, the use of a larger value of the strong coupling ($\alpha_s^{\text{ZGC}} = 0.26$), which would increase our cross section at a fixed value of the K factor by about 53%, the use of a smaller value of the electromagnetic coupling ($\alpha^{\text{ZGC}} = 1/137$), which would decrease our cross section by about 9%, the use of a larger value of the charm-quark mass ($m_c^{\text{ZGC}} = 1.5$ GeV), which would decrease our cross section at fixed values of the NRQCD matrix elements by about 19%, and the use of smaller values of $\langle \mathbf{q}^2 \rangle_{J/\psi}$ and $\langle \mathbf{q}^2 \rangle_{\eta_c}$, which would decrease our cross section by about 16%.

In Ref. [10], the dependence of the cross section on m_c is given. A dependence is found that is slightly larger in magnitude (37% versus 30%) but opposite in sign to the one that we find. Presumably the difference arises because, in the method that is used to determine $\langle \mathcal{O}_1 \rangle_{J/\psi}$ and $\langle \mathcal{O}_1 \rangle_{\eta_c}$ in Ref. [10], those quantities are proportional to m_c^2 . In the method that is used in Ref. [11] to determine $\langle \mathcal{O}_1 \rangle_{J/\psi}$ and $\langle \mathcal{O}_1 \rangle_{\eta_c}$, the dependence of those quantities on m_c is much milder, partly because some factors of $2m_c$ are replaced with $m_{J/\psi}$. The authors of Ref. [10] have not estimated the sizes of uncertainties that arise from other sources, and so it is not clear whether their method of calculation leads to a more precise prediction for the cross section than the one that we have used.

XIII. SUMMARY AND DISCUSSION

For a number of years, the discrepancy between theoretical predictions for the exclusive double-charmonium cross section $\sigma[e^+e^- \rightarrow J/\psi + \eta_c]$ and experimental measurements has posed a significant challenge to our understanding of quarkonium production. Changes in

the measured values of the cross section have reduced the discrepancy somewhat [5, 6]. More recently, calculations of the corrections of NLO in α_s [7] and relativistic corrections [9, 10] have increased the theoretical prediction for the cross section by almost an order of magnitude. The shifts in the theoretical and experimental central values for the cross section have resolved the outstanding discrepancy. However, in the absence of an analysis of the theoretical uncertainties, the meaning of the apparent agreement between theory and experiment is unclear.

In this paper, we have carried out a new computation of the relativistic corrections to $\sigma[e^+e^- \rightarrow J/\psi + \eta_c]$, with the goals of adding certain refinements to the calculation and making a more precise estimate of the theoretical uncertainties. Some of the refinements, relative to the calculation of Ref. [9], are the use of the VMD method to calculate the fragmentation contribution to the pure QED amplitude, the inclusion of the effects of the running of α , and the inclusion of a precise calculation of the interference between the relativistic corrections and the corrections of NLO in α_s , as opposed to the use of a simple K -factor estimate. A further significant refinement in our calculation is the use of an improved determination of the relevant NRQCD matrix elements at leading order in v^2 and at NLO in v^2 (Ref. [11]). This determination includes an analysis of the correlated uncertainties in the matrix elements. Our calculation exploits this information to give a much more complete estimate of the uncertainties than was given in Ref. [9].

Our calculation differs from the one in Ref. [10] in that we include pure QED corrections, we take into account the effects of the running of α , we include the interference between the relativistic corrections and the corrections of NLO in α_s , and we resum a class of relativistic corrections. As we discuss in Section XII, the calculation of Ref. [10] makes use of matrix elements that differ significantly in numerical value from those that we use. Ref. [10] includes a discussion of scale uncertainties and the effect of the uncertainty in m_c , but does not provide an overall error bar for the cross section.

In our calculation, the relativistic corrections to $\sigma[e^+e^- \rightarrow J/\psi + \eta_c]$ arise from two sources. The first, direct source consists of the relativistic corrections to the process $e^+e^- \rightarrow J/\psi + \eta_c$ itself. These increase the cross section by about 40%. The second, indirect source of relativistic corrections derives from the relativistic corrections to the electromagnetic decay widths of the J/ψ and the η_c , which enter into the matrix-element determinations of Ref. [11]. This source increases the cross section by about 88% (Ref. [11]). (Other, smaller corrections

result in a net change in $\langle \mathcal{O}_1 \rangle_{J/\psi} \langle \mathcal{O}_1 \rangle_{\eta_c}$ of 71% relative to the value of $\langle \mathcal{O}_1 \rangle_{J/\psi} \langle \mathcal{O}_1 \rangle_{\eta_c}$ that was used in the calculation of Ref. [3].) The inclusion of corrections of NLO in α_s further increases the cross section by about 89%, of which about 15% comes from the interference between the relativistic corrections and the corrections of NLO in α_s .

Our principal results are given in Eqs. (50) and (51). In the former result, the uncertainties that arise from uncalculated higher-order corrections are estimated by varying the renormalization scale. In the latter result, those uncertainties are assumed to be given by their nominal sizes, namely, α_s^2 and $\alpha_s v^2$ times the cross section. In addition, there are uncertainties that result from the use of the NRQCD factorization formula for the cross section, which we estimate to be about 34%.

The central value for $\sigma[e^+e^- \rightarrow J/\psi + \eta_c]$ that we obtain is essentially the same as that of Ref. [9]. The effects of the various refinements that we have mentioned largely cancel. However, some of the refinements allow us to constrain the theoretical uncertainties more tightly. Because we have included more sources of uncertainty in our estimates, our error bars are significantly larger than those in Ref. [9].

Our results for $\sigma[e^+e^- \rightarrow J/\psi + \eta_c]$ also agree, within uncertainties, with the result of Ref. [10]. To some extent, the effects of our use of different values of the matrix elements and other input parameters are canceled by our inclusion of additional corrections. In Ref. [10], the dependence of the cross section on m_c is given. That dependence is similar in magnitude but opposite in sign to the one that we find, presumably because the authors of Ref. [10] use a method to determine the NRQCD matrix elements that is quite different from the method in Ref. [11]. The authors of Ref. [10] have not estimated other uncertainties, and so it is not clear whether their method of calculation yields a result that is more precise or less precise than ours.

As we have mentioned, in our calculation, we resum a class of relativistic corrections to all orders in v . These corrections include all of the relativistic corrections that are contained in the color-singlet $Q\bar{Q}$ quarkonium wave function, up to the ultraviolet cutoff of the NRQCD matrix elements. The effect of the resummation beyond relative order v^2 is small, indicating that the velocity expansion converges well for this process. The fact that the direct relativistic corrections are modest in size supports the conclusion in Ref. [18] that the effects of the finite width of the momentum-space $Q\bar{Q}$ wave function are small, once one excludes contributions from the large-momentum tails of the wave function that are

contained in corrections of higher order in α_s .

Let us discuss the prospects for decreasing the uncertainties in our calculation. The largest uncertainty arises from the uncalculated terms of relative order $\alpha_s v^2$ and relative order α_s^2 . This uncertainty may be as large as $^{+42\%}_{-30\%}$. A complete calculation of the order- $\alpha_s v^2$ corrections, which are the larger ones, seems quite feasible. The calculation of the corrections of order- α_s^2 would be a major undertaking, but is not out of the question. The next largest source of uncertainty arises from the use of the NRQCD factorization formalism itself, which may lead to an uncertainty of about 34%. A more thorough understanding of the issues that are involved in constructing a rigorous proof of a factorization theorem for $\sigma[e^+e^- \rightarrow J/\psi + \eta_c]$ may lead to a different estimate of these uncertainties. It is also conceivable that one could prove a “higher-twist” factorization theorem that would allow one to carry out a systematic computation of corrections to the existing NRQCD factorization formula. The uncertainties that arise from the use of the NRQCD factorization formalism presumably would decrease as the CM energy of the process $e^+e^- \rightarrow J/\psi + \eta_c$ increases. However, there are no prospects for measuring $\sigma[e^+e^- \rightarrow J/\psi + \eta_c]$ at higher energies in the immediate future. The uncertainty in m_c is the next most important source of theoretical uncertainty. We estimate the resulting uncertainty in the cross section to be $^{+30\%}_{-21\%}$. We can expect to see some progress in reducing this uncertainty, particularly from lattice determinations of m_c .

Our result for $\sigma[e^+e^- \rightarrow J/\psi + \eta_c]$ agrees, within errors, with the measurements of the Belle and BABAR experiments. The uncertainties in our result are quite large, and, of course, it would be desirable to reduce these uncertainties, so as to sharpen this test of the NRQCD factorization approach to quarkonium production. Nevertheless, it seems fair to conclude that the long-standing discrepancy between the theoretical prediction for $\sigma[e^+e^- \rightarrow J/\psi + \eta_c]$ and the experimental measurements has been resolved.

Acknowledgments

We thank Kuang-Ta Chao for providing us with numerical values of the NLO cross section for various values of the input parameters. We are grateful to Jens Erler for providing us with the latest version of the code GAPP and for explaining its use. We also thank Taewon Kim for checking the central value of the cross section. JL thanks the High Energy

Physics Theory Group at Argonne National Laboratory for its hospitality while this work was carried out. Work in the High Energy Physics Division at Argonne National Laboratory is supported by the U. S. Department of Energy, Division of High Energy Physics, under Contract No. DE-AC02-06CH11357. The work of JL was supported by the Korea Research Foundation under MOEHRD Basic Research Promotion grant KRF-2004-015-C00092 and by a Korea University Grant. The work of CY was supported by the Korea Research Foundation under MOEHRD Basic Research Promotion grant KRF-2006-311-C00020.

-
- [1] K. Abe *et al.* [Belle Collaboration], Phys. Rev. Lett. **89**, 142001 (2002) [arXiv:hep-ex/0205104].
 - [2] G. T. Bodwin, E. Braaten, and G. P. Lepage, Phys. Rev. D **51**, 1125 (1995) [Erratum-ibid. D **55**, 5853 (1997)] [arXiv:hep-ph/9407339].
 - [3] E. Braaten and J. Lee, Phys. Rev. D **67**, 054007 (2003) [Erratum-ibid. D **72**, 099901 (2005)] [arXiv:hep-ph/0211085].
 - [4] K. Y. Liu, Z. G. He, and K. T. Chao, Phys. Lett. B **557**, 45 (2003) [arXiv:hep-ph/0211181].
 - [5] K. Abe *et al.* [Belle Collaboration], Phys. Rev. D **70**, 071102 (2004) [arXiv:hep-ex/0407009].
 - [6] B. Aubert *et al.* [BABAR Collaboration], Phys. Rev. D **72**, 031101 (2005) [arXiv:hep-ex/0506062].
 - [7] Y. J. Zhang, Y. j. Gao, and K. T. Chao, Phys. Rev. Lett. **96**, 092001 (2006) [arXiv:hep-ph/0506076].
 - [8] G. T. Bodwin, D. Kang, and J. Lee, Phys. Rev. D **74**, 014014 (2006) [arXiv:hep-ph/0603186].
 - [9] G. T. Bodwin, D. Kang, T. Kim, J. Lee, and C. Yu, AIP Conf. Proc. **892**, 315 (2007) [arXiv:hep-ph/0611002].
 - [10] Z. G. He, Y. Fan, and K. T. Chao, Phys. Rev. D **75**, 074011 (2007) [arXiv:hep-ph/0702239].
 - [11] G. T. Bodwin, H. S. Chung, D. Kang, J. Lee, C. Yu, arXiv:0710.0994 [hep-ph].
 - [12] G. T. Bodwin and A. Petrelli, Phys. Rev. D **66**, 094011 (2002) [arXiv:hep-ph/0205210].
 - [13] G. T. Bodwin, E. Braaten, J. Lee, and C. Yu, Phys. Rev. D **74**, 074014 (2006) [arXiv:hep-ph/0608200].
 - [14] W. M. Yao *et al.* [Particle Data Group], “Review of particle physics,” J. Phys. G **33**, 1 (2006) (m_{η_c} is taken from “The 2007 updates of the Particle Listings” at <http://pdg.lbl.gov>).
 - [15] J. Erler, Phys. Rev. D **59**, 054008 (1999) [arXiv:hep-ph/9803453]; arXiv:hep-ph/0005084.

- [16] K. T. Chao, private communications.
- [17] See, for example, G. C. Nayak, J. W. Qiu, and G. Sterman, Phys. Rev. D **72**, 114012 (2005) [arXiv:hep-ph/0509021].
- [18] G. T. Bodwin, D. Kang, and J. Lee, Phys. Rev. D **74**, 114028 (2006) [arXiv:hep-ph/0603185].